

# UC San Diego

## UC San Diego Previously Published Works

### Title

High-throughput lipidomic analysis of fatty acid derived eicosanoids and N-acylethanolamines

### Permalink

<https://escholarship.org/uc/item/5qm1p1rd>

### Journal

Biochimica et Biophysica Acta, 1811(11)

### ISSN

0006-3002

### Authors

Dumlao, Darren S  
Buczynski, Matthew W  
Norris, Paul C  
[et al.](#)

### Publication Date

2011-11-01

### DOI

10.1016/j.bbalip.2011.06.005

Peer reviewed

Published in final edited form as:

*Biochim Biophys Acta*. 2011 November ; 1811(11): 724–736. doi:10.1016/j.bbaliip.2011.06.005.

## High-Throughput Lipidomic Analysis of Fatty Acid Derived Eicosanoids and N-Acylethanolamines

Darren S. Dumlao<sup>\*</sup>, Matthew W. Buczynski<sup>\*</sup>, Paul C. Norris, Richard Harkewicz, and Edward A. Dennis

Department of Chemistry and Biochemistry and Departments of Pharmacology, University of California, San Diego, La Jolla, CA 92093

### 1. Introduction

Eicosanoids and N-acylethanolamines (NAEs) are very important bioactive lipid molecules that signal numerous physiological processes [1, 2]. Comprehensive metabolomic tools to study these lipids and their biological involvement have been challenging since lipids represent a very diverse group of molecules comprised of many different classes and subclasses [3]. Additionally, each subclass has many distinct chemical features making it very difficult to monitor every type of lipid in a single analysis. LIPID Metabolites And Pathways Strategy (LIPID MAPS), a NIH-funded consortium was created to develop the infrastructure required including the specific methodology reported herein, an extensive lipid database, and to develop lipid standards ([www.lipidmaps.org](http://www.lipidmaps.org)).

Eicosanoids and NAEs comprise two classes of important bioactive lipid signaling molecules that act through binding to their cognate receptors. Eicosanoids and NAEs play a key role in the innate immune system modulating inflammation, cellular recruitment, pain signaling, blood pressure response, and fever [1, 2]. Additionally, many of these lipid metabolites have been implicated in a wide range of complex disease pathologies including cancer [4, 5], atherosclerosis [6], rheumatoid arthritis [7], cystic fibrosis [8] and neurodegeneration [9].

Eicosanoids represent a large diverse group of lipids, in part, due to nonspecific synthases that can utilize different polyunsaturated fatty acids (PUFA) as substrates. The complexity of the eicosanoids is further complicated because these molecules can then act as substrates for other synthases, either through an intracellular or trans-cellular mechanism [2, 10]. They are derived from polyunsaturated fatty acids (typically arachidonic acid) located at the sn-2 position of membrane glycerophospholipids liberated by enzymes with phospholipase A<sub>2</sub> (PLA<sub>2</sub>) activity [11, 12]. Group IVA cPLA<sub>2</sub> has been thought to be the main phospholipase responsible for the fatty acyls liberated from membrane phospholipids, while a recent report suggest that MAGL is the main lipase responsible for this activity in brain [13, 14]. These free fatty acyls serve as substrates for cyclooxygenases (COX), lipoxygenases (LOX), and cytochrome P450s (CYP) enzymes [1, 2, 15, 16]. Most eicosanoid studies have just focused

© 2011 Elsevier B.V. All rights reserved.

Address correspondence to: Edward A. Dennis, 4076 Biomedical Science Building, University of California, San Diego, CA 92095. Tel.: 858-534-3055, Fax: 858-534-7390; [edennis@ucsd.edu](mailto:edennis@ucsd.edu).

<sup>\*</sup>These authors contributed equally

**Publisher's Disclaimer:** This is a PDF file of an unedited manuscript that has been accepted for publication. As a service to our customers we are providing this early version of the manuscript. The manuscript will undergo copyediting, typesetting, and review of the resulting proof before it is published in its final citable form. Please note that during the production process errors may be discovered which could affect the content, and all legal disclaimers that apply to the journal pertain.

on prostaglandin E<sub>2</sub> (PGE<sub>2</sub>) and the role it plays in inflammatory responses. Since many eicosanoids display redundant signaling properties, efforts have been made to study these mediators collectively.

NAEs represent a class of endogenous bioactive signaling lipids composed of a fatty acyl conjugated to ethanolamine through the amide bond [17, 18]. The arachidonoyl species, anandamide (AEA), has received the most attention due to its anti-inflammatory action, nearly all endogenous fatty acyl species have been detected as ethanolamides *in vivo* [19]. A number of different pathways have been implicated in NAE formation, but the specific enzymes generating synaptic AEA formation remains unclear. To date, three main enzymatic routes for the formation of AEA from n-acyl phosphatidylethanolamines (NAPE) have been identified: (1) hydrolysis by a NAPE-specific phospholipase D (NAPE-PLD), (2) sequential phospholipase A/B activity of ABHD4, followed by a metal-dependent phosphodiesterase, and (3) sequential phospholipase C (PLC) and phosphatase activity. Inactivation of NAE signaling occurs primarily through their hydrolysis to form the free fatty acids and ethanolamine. Fatty acid acyl hydrolase (FAAH) has been identified as the primary means of AEA metabolism through a well-characterized serine hydrolase mechanism. Predominately, FAAH associates with intracellular membranes such as the endoplasmic reticulum and the Golgi apparatus. A great number of small molecules have been developed as selective inhibitors of FAAH [20-23], which has been a hotly pursued pharmacological target.

The quantitation of eicosanoids has been a challenging task due to the number of chemically different yet structurally similar metabolites (over 100). In the past, enzyme-linked immunosorbent assays (EIA) were employed to monitor a single eicosanoid species [24, 25]. Due to the lack of commercially available antibodies and their non-specificity, this approach was severely limited. Additionally, the EIA approach lacked the robustness to perform large scale analyses. The technological advancements in mass spectrometry and its application to monitor eicosanoids have led to a robust foundation for eicosanoid research. Using gas chromatography mass spectrometry (GC/MS) allowed for many eicosanoids to be monitored simultaneously, however, a lone chemical derivatization agent was not suitable for all eicosanoids to be monitored in a single analysis [26]. Also, GC/MS was not suited for monitoring every type of eicosanoid species [27]. Electrospray-ionization tandem mass spectrometry (ESI-MS/MS), which does not require a prior derivatization step, has become a staple in eicosanoid biology since it was first employed by Margalit and colleagues for simultaneously monitoring 14 different eicosanoid species in a single analysis [28]. The number of distinct eicosanoids that can be monitored in a single analysis has been steadily increasing as more pure standards have become commercially available, as well as improvements in mass spectrometer hardware and data analysis software.

Previously, we reported on the use of GC/MS to analyze free fatty acids [29] and LC/MS/MS to analyze eicosanoids [30]. Our initial eicosanoid methodology was capable of monitoring 60 unique species in a single 16 min analysis. Since our initial report, significant improvements have been made which more than doubles the number of eicosanoids monitored (141) and quantified (100). Additionally, we have applied this technique toward a separate methodology capable of monitoring 36 NAE metabolites. Here, we present the design and rationale behind our high-throughput LC/MS/MS methodologies for monitoring and quantitating eicosanoid and NAE metabolites, and highlight the improvements made over our previous technique. Also, we provide an example of the application of our methodology.

## 2. Materials and Methods

### 2.1. Sample Preparation

The same sample preparation is used when analyzing eicosanoids or NAEs. All samples were resuspended in 1.0 ml of 10% methanol water (v/v). Tissue samples were subjected to sonication for 6 seconds to break up any connective tissue. Samples were spiked with 50  $\mu\text{L}$  of a 50 pg/ $\mu\text{L}$  (2.5 ng total) deuterated internal standard solution. Lipid metabolites were extracted using strata-x 33  $\mu$  polymerized solid reverse phase extraction columns (Phenomenex, CA; cat # 8B-S100-UBJ) as indicated by manufacturer's directions. Briefly, columns were washed with 3.5 ml of 100% methanol, followed by 3.5 ml of water before samples were extracted. Samples were washed with 3.5 ml of 10% methanol to remove non-specific binding metabolites. Lipids were eluted into 1.0 ml of methanol and stored at  $-80^{\circ}\text{C}$  before being analyzed to prevent metabolite degradation.

### 2.2. High performance liquid chromatography (HPLC)

Both eicosanoid and NAE samples are subjected to the same treatment for HPLC analysis, although different buffer systems are employed. Extracted samples in 100% methanol are lyophilized to dryness using a speed-vac concentrator (Savant, model # SC110-120), and resuspended in 90  $\mu\text{L}$  of their respective solvent A. For the eicosanoids methodology, solvent  $\text{A}_{\text{EICOS}}$  consists of water-acetonitrile-acetic acid (70:30:0.02; v/v/v), while solvent  $\text{B}_{\text{EICOS}}$  consists of acetonitrile-isopropyl alcohol (50:50, v/v). For the NAE methodology, solvent  $\text{A}_{\text{NAE}}$  consists of water-acetonitrile-acetic acid ((70:30:0.1; v/v/v) + 1 g/L ammonium acetate) and solvent  $\text{B}_{\text{NAE}}$  consists of acetonitrile-isopropyl alcohol-acetic acid ((45:45:10; v/v/v) + 1 g/L ammonium acetate). Samples can be subjected to each methodology alone or analyzed together in series. After a sample has been analyzed for eicosanoids, the presence of NAEs can be determined with the addition of 10  $\mu\text{L}$  of a water-acetonitrile-acetic acid (70:30:0.1; v/v/v) + 5 g/L ammonium acetate solution that makes the sample suitable to be analyzed in positive-ion mode.

An aliquot of 40  $\mu\text{L}$  of sample injected on the HPLC system was the standard amount routinely analyzed. Eicosanoids were separated on a Synergi reverse-phase C18 column (2.1  $\times$  250 mm; Phenomenex, CA) and NAEs were separated on a Luna reverse-phase C8 column (2.1 mm  $\cdot$  250 mm, Phenomenex, CA). Both sample types use a flow rate of 300  $\mu\text{L}/\text{min}$  at  $50^{\circ}\text{C}$ . The gradient program used to separate the eicosanoids is as follows: 1 min (0% solvent  $\text{B}_{\text{EICOS}}$ ), 3 min (25% solvent  $\text{B}_{\text{EICOS}}$ ), 11 min (45% solvent  $\text{B}_{\text{EICOS}}$ ), 13 min (60% solvent  $\text{B}_{\text{EICOS}}$ ), 18 min (75% solvent  $\text{B}_{\text{EICOS}}$ ), 18.5 min (90% solvent  $\text{B}_{\text{EICOS}}$ ), 20 min (90% solvent  $\text{B}_{\text{EICOS}}$ ), 21 min (0% solvent  $\text{B}_{\text{EICOS}}$ ). A linear gradient was maintained between each step. The column was re-equilibrated by holding 0% solvent  $\text{B}_{\text{EICOS}}$  between min 21 to 25 before the next sample injection. The gradient program used to separate the NAEs is as follows: 1 min (0% solvent  $\text{B}_{\text{NAE}}$ ), 4 min (50% solvent  $\text{B}_{\text{NAE}}$ ), 14 min (100% solvent  $\text{B}_{\text{NAE}}$ ), 20 min (100% solvent  $\text{B}_{\text{NAE}}$ ), and 21 min (0% solvent  $\text{B}_{\text{NAE}}$ ). A linear gradient was maintained between each step. The column was re-equilibrated by holding 0% solvent  $\text{B}_{\text{NAE}}$  between min 21 to 25 before the next sample injection.

### 2.3. Mass Spectrometry

An ABI/Sciex (Foster City, CA) 4000 QTRAP hybrid, triple quadrupole, linear ion trap mass spectrometer equipped with a Turbo V ion source was used for all mass spectrometry analysis. Analyst 1.5 software package was used to operate the mass spectrometer. Nitrogen gas was used as the collision gas for all metabolites. Eicosanoids were detected in negative electrospray ion mode with the following source parameters: CUR = 10 psi, GS1 = 30psi, GS2 = 30 psi, IS = -4500 V, CAD = HIGH, TEMP =  $525^{\circ}$ , ihe = ON, EP = -10 V, and CXP = -10 V. NAEs were analyzed in positive electrospray ion mode with the following source

parameters: CUR = 10 psi, GS1 = 30psi, GS2 = 30 psi, IS = -4500 V, CAD = HIGH, TEMP = 525°, ihe = ON, EP = -10 V, and CXP = -10 V.

## 2.4. Quantitation

Eicosanoids and NAEs are quantitated using a stable isotope dilution technique. Primary standard curves are produced separately for eicosanoids and NAEs. Primary standard curves are generated from mixed primary standard stocks at 7 different concentrations (0.1 ng, 0.3 ng, 1 ng, 3 ng, 10 ng, 30 ng, and 100 ng). An aliquot of 50 mL of primary standard stock with the concentration ranging from 1 pg/μL (0.1 ng stock) to 1000 pg/μL (100 ng) are added to an aliquot of 25 μL of internal standard stock. For eicosanoids, 75 μL of 0.2% acetic acid-water were added, while for NAEs 75 μL of solvent A<sub>NAE</sub> (water-acetonitrile-acetic acid (70:30:0.1; v/v/v) + 1 g/L ammonium acetate). A 40 μL aliquot of each primary standard mix is analyzed with mass spectrometric methodologies. Primary standards were run in duplicate and averaged. Primary standard curves are determined by generating a linear regression trend line that is forced through 0. The multiquant 1.1 software package (ABI-Sciex) was used to quantitate all metabolites.

## 3. Rationale and Discussion

### 3.1. Sample preparation

These methodologies have been applied to media from cultured primary cells, cultured cell lines (RAW264.7 and HEK293) [31], rat spinal cord tissue [19], murine papillomas, and murine tibiotarsal ankle joints [32]. The same sample preparation is used when analyzing eicosanoids or NAEs. All tissue samples were disrupted with a probe sonicator, while murine papilloma tissue required homogenization prior to sonication. Lipid metabolites were isolated from cultured media and tissue samples using solid phase extraction, except for murine ankle joints where a prior liquid / liquid extraction was employed [32]. A murine ankle joint sample is comprised mostly of bone and required an additional total lipid extraction.

Purification using flash chromatography can significantly enhance lipid detection and quantization limits by removing other chemical species that can diminish the overall sensitivity through processes such as ion suppression. Different extraction methods have been employed in the study of these lipid mediators [33, 34]. We decided to use a solid phase extraction technique, which is more suitable for processing a large number of samples than a more efficient liquid/liquid extraction technique as described in Golovko *et al.*, 2008 [33]. The solid phase extraction technique utilizes Strata-x polymerized solid reverse phase extraction columns (Phenomenex, CA; cat # 8B-S100-UBJ). Samples are applied to these columns in 10% methanol, a concentration of organic solvent empirically determined to be sufficient to solubilize the eicosanoids and NAEs in our assay, yet not high enough to prevent them from binding to the column. An additional column volume of 10% methanol is used as a wash, which serves to elute non-specific hydrophobic chemical species and salts from the sample. Subsequently, eicosanoids and NAEs are eluted off the column with 100% of methanol; however, a large fraction of the more lipophilic species that could potentially lead to ion suppression is retained. Previously, our lab has reported on some lipid recoveries obtained from this extraction technique [30]. Lipids are stored in 100% methanol at -80°C to minimize non-enzymatic oxidation and degradation until analysis.

A crucial aspect of our methodology is the usage of deuterated internal standards. All samples are spiked with a deuterated internal standard solution prior to lipid extraction. The use of deuterated internal standards is intrinsic to our ability to quantitate these lipids, and is covered in greater depth in the quantitation section (3.5). Deuterated internal standards also

serve an important role in the extraction and storage process. Since a deuterated internal standard is either an analogous lipid metabolite or a molecule with similar chemical characteristics, both lipid metabolite and internal standard will have similar extraction efficiencies and rates of degradation. Thus, any amount of a lipid metabolite that is lost due to the extraction process or degradation will be accounted for.

### 3.2. Method design

Our methodology uses a targeted approach to identify and quantitate lipids using mass spectrometry (MS) coupled with high performance liquid chromatography (HPLC). This approach is known as the Comprehensive Lipidomic Analysis by Separation Simplification (CLASS) [3], where lipid metabolites are separated based on their chemical properties prior to mass analysis, then monitored by collision-induced decomposition (CID) in conjunction with electrospray ionization tandem mass spectrometry (ESI-MS/MS) [3]. Using CID, whereby each lipid metabolite creates ion fragments unique to its structural components, they can be subsequently measured by monitoring one of these ion fragments. A targeted MS approach allows for a higher sensitivity to detect analytes than an unbiased full scan MS analysis. The trade off for higher sensitivity is that novel metabolites cannot be detected, and all metabolites of interest must be accounted for prior to analysis.

Mass spectrometric analysis was performed on an ABI/Sciex 4000 Q-TRAP operating in scheduled multiple-reaction monitoring (sMRM) mode. Multiple-reaction monitoring (MRM) is a MS approach that monitors the transition of a parent ion to a specific daughter ion fragment. PGE<sub>2</sub> and anandamide are used as examples to demonstrate the parent to daughter ion transition (Fig. 1). These defined parent and daughter ions are known as an MRM pair. An sMRM pair is an MRM pair with an associated liquid chromatography (LC) retention time. sMRM is an improvement over MRM allowing for better data collection and more analytes to be monitored in a single analysis. The MS operating software (Analyst 1.5) takes into account the total number of sMRM pairs and respective retention times, and optimizes how the mass spectrometer scans. We found that a 70 second retention time window for each sMRM pair was sufficient to account for metabolite peaks and slight shifts in their retention times. Although a feature on ABI/Sciex mass spectrometers running Analyst 1.5, scheduling MRM pairs can be replicated on triple quadrupole mass spectrometers from other companies. This method is intended as a starting point for the research community, which can be expanded upon as more metabolite standards become available, or scaled down to only include the metabolites of interest.

The switch from using MRM pairs to sMRM pairs has allowed us to increase the total number of metabolites monitored in our methodology, without sacrificing the quality of the data collected. Our previous eicosanoid methodology utilized manually dividing the entire mass spectrometric scan into 6 different 3-5 min periods, which contained about 20-30 metabolites with similar retention times. During each period, the mass spectrometer only monitored the contained subset of eicosanoids. This was done to maintain a duty cycle of less than 2 seconds. As more metabolites became available and added to the screen, it became a very laborious task to maintain an adequate duty cycle. Additionally, slight shifts in metabolite retention times due to column usage and variations in buffer preparations made it difficult to create and manage new periods. This methodology remained manageable as long as an upper limit of about 125 total MRM pairs was maintained. Our current eicosanoid methodology contains 171 total sMRM with improved sensitivity, where mass spectrometer algorithms have optimized the data collection process. These improvements are further discussed in the eicosanoid methodology and quantitation sections.



### 3.3. Eicosanoid methodology

We have developed a high-throughput CLASS approach to globally monitor a specific lipid class, the eicosanoids. Derived from poly-unsaturated fatty acids (PUFAs), all eicosanoids contain a conserved terminal carboxyl moiety (Fig. 1, PGE<sub>2</sub>). Eicosanoid are detected in negative electrospray ion mode to take advantage of the terminal carboxyl moiety, which is easily deprotonated during ionization. This feature allows eicosanoids to be detected without any additional derivatization. Unique sMRM pairs have been selected for each eicosanoid species. This was accomplished by analyzing product ion scans (MS/MS) from commercial eicosanoid standards (Cayman Chemical & Biomol). Additionally, optimal declustering potential (DP) and the collision energy (CE) parameters have been determined for each sMRM pair. These values were determined by directly infusing commercial standards into the mass spectrometer, while individually ramping these parameters in a MRM experiment. We have compiled the sMRM pair, DP, and CE values for each eicosanoid (Table 1). Table 1 also includes the biosynthetic pathway and PUFA that each eicosanoid is derived from.

Metabolite identification is achieved by combining both ESI-MS/MS and HPLC analyses. The detection of an sMRM pair with an associated retention time from a reverse-phase HPLC gradient for a particular lipid metabolite is matched to values obtained from a pure commercial standard subjected to the same LC/MS/MS analysis. Since chromatography fluctuates with column usage and variations in buffer preparation, it is imperative that eicosanoid standards are analyzed as part of every experiment. Our methodology contains 171 sMRM pairs (141 metabolites + 30 deuterated internal standards) for eicosanoids and related metabolites, which are monitored in a single 25 min LC/MS/MS analysis. Representative retention time values for each eicosanoid are reported in Table 1. Representative retention times are reported because retention fluctuations occur between experiments which can be due to column usage, buffer preparation, and instrument variation. A chromatograph from a single analysis of a 100 ng primary standard solution containing a total of 102 eicosanoid species demonstrates the robustness of our methodology (Fig. 2A). Specific eicosanoid ion chromatographs have been extracted to illustrate different features of our methodology (Fig. 2B). Chromatographic separation is paramount when monitoring a large number of structurally similar metabolites. The COX pathway derived metabolites, prostaglandin E<sub>2</sub> (PGE<sub>2</sub>) and prostaglandin D<sub>2</sub> (PGD<sub>2</sub>) have the same molecular formula, differing only by the placement of a keto- and hydroxyl- group at position 9 and 11. Subsequent full MS/MS scan analyses of these two molecules produce the exact same ion fragmentation pattern. The use of mass spectrometry alone is not sufficient to distinguish between metabolites that share the same sMRM pair. Adequate chromatographic separation of PGE<sub>2</sub> and PGD<sub>2</sub> allows us to differentiate between these two metabolites (Fig. 2B). There are 39 occurrences in our eicosanoid methodology where a metabolite shares an sMRM pair with another metabolite.

Adequate chromatographic separation is not always achieved, due to the high amount of structural similarity between eicosanoid species. Many eicosanoids have slight modifications to their molecular structure, while maintaining the exact molecular weight. This is exemplified in the lipoxygenase generated HETE (20-carbon) and HODE (18-carbon) metabolites that differ at the position of a single hydroxyl group. Our HPLC gradient produces only minimal chromatographic separation of these metabolites, leading to overlap of their elution profiles (Fig. 2C). These metabolites produce many of the same daughter ion fragments, making it difficult to distinguish each eicosanoid species using a full MS/MS scan. Our methodology overcomes this obstacle by utilizing a unique sMRM pair for each of these lipid metabolites. Our sMRM approach is able to detect which metabolites are present, even when a cluster of metabolites display overlapping elution profiles (Fig. 2C).

### 3.4. N-acylethanolamine (NAE) methodology

A similar CLASS approach used to monitor eicosanoids is employed in the detection of NAEs. The NAE methodology can be employed as a lone analysis or performed in tandem after samples have subjected to the eicosanoid methodology. All NAEs contain an acyl linkage to the nitrogen of an ethanolamine molecule (Fig. 1, AEA). NAEs are detected in positive electrospray ion mode. Unlike the eicosanoids, NAEs ionize more efficiently in positive ion mode due to their conserved amide nitrogen. Since the carboxyl-amide bond is labile, fragmentation of an N-acylethanolamine  $[M+H]^+$  species produces a 62 m/z ion ( $C_2H_8N_1O_1^+$ ). The presence of salts such as  $Na^+$  and  $K^+$ , which can remain associated with these lipids even after sample preparation, can facilitate the formation of other NAE ion species such as  $[M+Na]^+$  and  $[M+K]^+$ , diminishing the overall sensitivity of these lipids. Ammonium acetate, when used in concentrations above 1 mM, can shift the equilibrium toward  $[M+NH_4]^+$  species, which degrade to  $[M+H]^+ + NH_3$  during ionization. Similarly to the eicosanoids, no additional chemical derivatization is required to monitor NAEs. The current NAE methodology monitors 36 different metabolites, derived from saturated fatty acids, mono- to poly-unsaturated fatty acids, and eicosanoids. Some of these metabolites can be purchased (Cayman Chemical), while others were synthesized in our laboratory by standard methods. The sMRM pair and representative retention time for each NAE have been determined in the same manner as the eicosanoids (Table 2). Fragmentation of the carboxyl-amide bond required the same declustering potential (50) and collision energy (40) values for all NAEs.

The NAE metabolites are identified using a 25 min LC/MS/MS analysis. The identity of detected NAE metabolites are confirmed against pure NAE standards subjected to the same LC/MS/MS analysis. A chromatograph from a 100 ng standard stock solution containing 33 NAEs subjected to this methodology is depicted in Fig. 3A. Selected metabolites have been extracted to simplify the data produced by this method (Fig. 3B). Since every NAE generates the daughter ion fragment (62 m/z)<sup>+</sup>, many of metabolites share the same MRM transition. This can be seen when examining the different HETE-EA and EET-EA species which all have a 346.0/62.0 sMRM transition (Fig. 3C). Having adequate chromatographic separation is key in distinguishing these metabolites from each other. There are 15 NAEs that have a shared sMRM pair.

### 3.5. Quantitation

Our current methodology allows for both relative and exact quantitation using a stable isotope dilution technique [35]. This technique applies for the quantitation of eicosanoids and NAEs. First, we employ measures to filter out aberrant signals from the dataset, whereby a detected peak is considered valid if the peak's height is 3-fold greater than the background noise. Peaks that do not meet this requirement are disregarded. Also, the addition of deuterated internal standards can add contaminating lipid metabolites to the sample, which arise from impurities in the standard. The deuterated internal standard is mass analyzed in every experiment, and contaminating peaks are subtracted from the samples.

Both relative and exact quantitation heavily relies upon making comparisons between the integrated areas of a given lipid metabolite and its corresponding internal standard ( $Area_{METABOLITE} / Area_{INSTD}$ ). The internal standard solution for the eicosanoids is comprised of 30 deuterated eicosanoids, while the NAE's internal standard solution contains 4 deuterated NAEs. The criteria used to pair a metabolite with a particular internal standard include: 1) matching the metabolite with the analogous deuterated species (PGD<sub>2</sub> and d<sub>4</sub>-PGD<sub>2</sub>), or 2) matching the metabolite with an internal standard that has a similar chemical structure and retention time (PGJ<sub>2</sub> and d<sub>4</sub>-15d-PGJ<sub>2</sub>). Table 1 and 2 lists the deuterated internal standards (highlighted in gray) and lipid metabolite they were paired with. This



ratio, which is established prior to lipid extraction, is maintained throughout the entire sampling process. This technique allows for accurate quantitation because lipid metabolites and corresponding internal standards have similar ionization efficiencies and will be equally affected by factors such as ion suppression. An important caveat is that the internal standard must be detectable above the background for quantitation.

Relative quantitation is determined by comparing the ratio ( $\text{Area}_{\text{METABOLITE}} / \text{Area}_{\text{INSTD}}$ ) between two different samples. This can be useful in monitoring how a single or a group of lipid metabolites change during different stages of a disease, or how these metabolic pathways are globally affected by pharmacological intervention. To quantitate the exact amount of a given metabolite in a sample, a primary standard curve generated from commercially bought standards is required. Primary standard curves for eicosanoids and NAE are generated separately. A primary standard curve is produced from 7 different concentrated eicosanoid or NAE standard solutions (0.1 ng, 0.3 ng, 1 ng, 3 ng, 10 ng, 30 ng, and 100 ng) that have been spiked with the internal standard solution. Since the primary standard and internal standard solutions are maintained in 100% ethanol, the addition of aqueous buffer is required to reproduce a metabolite's chromatographic retention time. For eicosanoids, an equal volume of 0.2% acetic acid-water is added to the primary / internal standard mixture, while an equal volume of water-acetonitrile-acetic acid (70:30:0.1; v/v/v) + 1 g/L ammonium acetate is added to the NAE primary / internal standard mixture. Each primary standard concentration is analyzed in duplicate and averaged. The primary standard curve is determined by generating a linear regression trend line that is forced through 0.

Representative primary standard curves from eicosanoid and NAE metabolites are shown to illustrate this technique (Fig. 4). These primary standard curves were generated from 3 separate experiments performed in duplicate spanning a 2-month period. Each standard curve displays a correlation value ( $R^2$  value) above 0.999 indicating the high reproducibility of this methodology. Exact quantitation of a metabolite in a given sample is determined by extrapolating the amount (X-axis value) from where the ratio ( $(\text{Area}_{\text{METABOLITE}} / \text{Area}_{\text{INSTD}})$ ; (Y-axis value)) intercepts the primary standard curve (Fig. 4). Alternately, the exact amount of a given lipid metabolite in a sample can be determined by dividing the ratio ( $\text{Area}_{\text{METABOLITE}} / \text{Area}_{\text{INSTD}}$ ) by the slope of the standard curve. We routinely quantitate about 100 eicosanoids out of the total 141 monitored in a single analysis. Our NAE methodology contains 33 quantifiable metabolites out of a total 36 monitored in a single analysis. Some metabolites are not quantitated because either a pure standard is not available (such as the dihomo-prostaglandins) or are routinely observed in very low abundance in experimental models that we have examined

Monitoring sMRM pairs instead of full MS/MS scans greatly increases the sensitivity of detection. A 100 ng mixture of standards containing eicosanoids or NAE were serially diluted and analyzed by our methodology to determine the lower limit of detection (LOD) for a portion of the routinely quantitated eicosanoids and NAEs. These values are detailed in Table 1 and 2. The LOD for the eicosanoids analyzed ranged between 0.1 pg -1 pg. This is a definite improvement over our previous method with reported LOD values ranging from 1 pg to 10 pg on average [30]. The LOD values for a majority of NAEs were detected at 0.1 pg, while in a few instances a higher LOD value was observed ranging from 10 pg – 1000 pg. The difference in sensitivity is due to the efficiency and stability of the parent to daughter ion transition.

### 3.6. Application of the lipidomic methodology

The application of these methodologies can be used to globally monitor the changes in eicosanoid and NAE metabolites in tissue samples. As an example, cerebral spinal fluid (CSF) and lumbar spinal cord sections from rats injected with the hyperalgesia-inducing

agent carrageenan in their hind paw were analyzed by both eicosanoid and NAE methodologies performed in series [19]. The version of eicosanoid methodology employed during this study monitored fewer eicosanoid species (124 sMRM). The data obtained from an extensive 24 h time-course experiment is graphed as a heat map to show the global representation of the relative changes of these metabolites (Fig. 5). The power of this approach can be seen in the emergent patterns from large complex data sets. The administration of peripheral carrageenan caused an increase in central levels of arachidonic acid-derived (AA) COX metabolites. Also, 12-LOX and corresponding dehydration metabolites were also observed to increase. There is an extensive amount of literature on the involvement of PGE<sub>2</sub> (COX metabolite) in central pain signaling, however, little is known about the role that 12-LOX metabolites play in this process. These observations could have been missed if only a single or select group of lipid metabolites was monitored. The capability to globally monitor these lipids has led to the identification of new bioactive mediators.

Distinct patterns are observed when comparing the eicosanoid and NAE profiles from the CSF and spinal cord samples. Fewer total lipid metabolites are detected in CSF samples, containing only a portion of the eicosanoids detected in spinal cord (Fig. 5). Also, NAEs are only detected in the spinal cord sample. Temporal patterns between lipid metabolites present in both samples are observed. Examination of quantitated amounts of PGE<sub>2</sub> exemplifies the temporal differences between CSF and spinal cord (Fig. 6). PGE<sub>2</sub> peaks at 4 h in CSF then returns to basal levels by 24 h. In contrast, PGE<sub>2</sub> levels begin to rise at later times in the spinal cord and remain elevated. Additionally, the NAE anandamide (20:4-EA) is observed to significantly increase at later time points in the spinal cord (Fig. 6).

#### 4. Summary

We present a targeted CLASS approach to globally monitor and quantitate eicosanoids and N-acyl ethanolamines. Our current eicosanoid methodology represents a distinct advance over our previous versions, increasing the total number of sMRM pairs monitored from 60 to 171. The introduction of scheduled MRM (sMRM) pairs, has allowed for the detection of more metabolites, and the number is only limited by the number of available lipid metabolite standards. The increase in the total metabolites monitored has not compromised the quality of the data collection process. Software advancements have allowed for greater sensitivity and removed a lot of the tediousness of monitoring a very large set of metabolites. This methodology facilitates more thorough metabolite studies and can easily be adapted to other metabolite classes.

#### Acknowledgments

This work was supported by the LIPID MAPS Large Scale Collaborative Grant GM069338 and by GM064611

#### References

1. Funk, CD. Science. Vol. 294. New York, N.Y: 2001. Prostaglandins and leukotrienes: advances in eicosanoid biology; p. 1871-1875.
2. Buczynski MW, Dumlao DS, Dennis EA. Thematic Review Series: Proteomics. An integrated omics analysis of eicosanoid biology. Journal of lipid research. 2009; 50:1015–1038. [PubMed: 19244215]
3. Harkewicz R, D EA. Application of Mass Spectrometry to Lipids and Membranes. Annual Review Biochemistry. 2011
4. Rodriguez-Antona C, Ingelman-Sundberg M. Cytochrome P450 pharmacogenetics and cancer. Oncogene. 2006; 25:1679–1691. [PubMed: 16550168]

5. Hyde CA, Missailidis S. Inhibition of arachidonic acid metabolism and its implication on cell proliferation and tumour-angiogenesis. *International immunopharmacology*. 2009; 9:701–715. [PubMed: 19239926]
6. Weitz D, Weintraub H, Fisher E, Schwartzbard AZ. Fish oil for the treatment of cardiovascular disease. *Cardiology in review*. 18:258–263. [PubMed: 20699674]
7. Calder PC, Zurier RB. Polyunsaturated fatty acids and rheumatoid arthritis. *Current opinion in clinical nutrition and metabolic care*. 2001; 4:115–121. [PubMed: 11224655]
8. Harmon GS, Dumlao DS, Ng DT, Barrett KE, Dennis EA, Dong H, Glass CK. Pharmacological correction of a defect in PPAR-gamma signaling ameliorates disease severity in Cfr-deficient mice. *Nature medicine*. 16:313–318.
9. Pierre SR, Lemmens MA, Figueiredo-Pereira ME. Subchronic infusion of the product of inflammation prostaglandin J2 models sporadic Parkinson's disease in mice. *Journal of neuroinflammation*. 2009; 6:18. [PubMed: 19630993]
10. Sala A, Folco G, Murphy RC. Transcellular biosynthesis of eicosanoids. *Pharmacol Rep*. 62:503–510. [PubMed: 20631414]
11. Six DA, Dennis EA. The expanding superfamily of phospholipase A(2) enzymes: classification and characterization. *Biochimica et biophysica acta*. 2000; 1488:1–19. [PubMed: 11080672]
12. Schaloske RH, Dennis EA. The phospholipase A2 superfamily and its group numbering system. *Biochimica et biophysica acta*. 2006; 1761:1246–1259. [PubMed: 16973413]
13. Nomura DK, Blankman JL, Simon GM, Fujioka K, Issa RS, Ward AM, Cravatt BF, Casida JE. Activation of the endocannabinoid system by organophosphorus nerve agents. *Nature chemical biology*. 2008; 4:373–378.
14. Long JZ, Nomura DK, Vann RE, Walentiny DM, Booker L, Jin X, Burston JJ, Sim-Selley LJ, Lichtman AH, Wiley JL, Cravatt BF. Dual blockade of FAAH and MAGL identifies behavioral processes regulated by endocannabinoid crosstalk in vivo. *Proceedings of the National Academy of Sciences of the United States of America*. 2009; 106:20270–20275. [PubMed: 19918051]
15. Simmons DL, Botting RM, Hla T. Cyclooxygenase isozymes: the biology of prostaglandin synthesis and inhibition. *Pharmacological reviews*. 2004; 56:387–437. [PubMed: 15317910]
16. Sacerdoti D, Gatta A, McGiff JC. Role of cytochrome P450-dependent arachidonic acid metabolites in liver physiology and pathophysiology. *Prostaglandins & other lipid mediators*. 2003; 72:51–71. [PubMed: 14626496]
17. Buczynski MW, Parsons LH. Quantification of brain endocannabinoid levels: methods, interpretations and pitfalls. *British journal of pharmacology*. 160:423–442. [PubMed: 20590555]
18. Ueda N, Tsuboi K, Uyama T. Enzymological studies on the biosynthesis of N-acylethanolamines. *Biochimica et biophysica acta*. 1801:1274–1285. [PubMed: 20736084]
19. Buczynski MW, Svensson CI, Dumlao DS, Fitzsimmons BL, Shim JH, Scherbart TJ, Jacobsen FE, Hua XY, Yaksh TL, Dennis EA. Inflammatory hyperalgesia induces essential bioactive lipid production in the spinal cord. *Journal of neurochemistry*. 114:981–993. [PubMed: 20492349]
20. Ahn K, Johnson DS, Mileni M, Beidler D, Long JZ, McKinney MK, Weerapana E, Sadagopan N, Liimatta M, Smith SE, Lazerwith S, Stiff C, Kamtekar S, Bhattacharya K, Zhang Y, Swaney S, Van Becelaere K, Stevens RC, Cravatt BF. Discovery and characterization of a highly selective FAAH inhibitor that reduces inflammatory pain. *Chem Biol*. 2009; 16:411–420. [PubMed: 19389627]
21. Karbarz MJ, Luo L, Chang L, Tham CS, Palmer JA, Wilson SJ, Wennerholm ML, Brown SM, Scott BP, Apodaca RL, Keith JM, Wu J, Breitenbucher JG, Chaplan SR, Webb M. Biochemical and biological properties of 4-(3-phenyl-[1,2,4] thiadiazol-5-yl)-piperazine-1-carboxylic acid phenylamide, a mechanism-based inhibitor of fatty acid amide hydrolase. *Anesth Analg*. 2009; 108:316–329. [PubMed: 19095868]
22. Wang X, Sarris K, Kage K, Zhang D, Brown SP, Kolasa T, Surowy C, El Kouhen OF, Muchmore SW, Brioni JD, Stewart AO. Synthesis and evaluation of benzothiazole-based analogues as novel, potent, and selective fatty acid amide hydrolase inhibitors. *J Med Chem*. 2009; 52:170–180. [PubMed: 19072118]

23. Piomelli D, Tarzia G, Duranti A, Tontini A, Mor M, Compton TR, Dasse O, Monaghan EP, Parrott JA, Putman D. Pharmacological profile of the selective FAAH inhibitor KDS-4103 (URB597). *CNS Drug Rev.* 2006; 12:21–38. [PubMed: 16834756]
24. Reinke M. Monitoring thromboxane in body fluids: a specific ELISA for 11-dehydrothromboxane B2 using a monoclonal antibody. *The American journal of physiology.* 1992; 262:E658–662. [PubMed: 1590375]
25. Shono F, Yokota K, Horie K, Yamamoto S, Yamashita K, Watanabe K, Miyazaki H. A heterologous enzyme immunoassay of prostaglandin E2 using a stable enzyme-labeled hapten mimic. *Analytical biochemistry.* 1988; 168:284–291. [PubMed: 3129960]
26. Baranowski R, Pacha K. Gas chromatographic determination of prostaglandins. *Mini reviews in medicinal chemistry.* 2002; 2:135–144. [PubMed: 12370075]
27. Murphy RC, Barkley RM, Zemski Berry K, Hankin J, Harrison K, Johnson C, Krank J, McAnoy A, Uhlson C, Zarini S. Electrospray ionization and tandem mass spectrometry of eicosanoids. *Analytical biochemistry.* 2005; 346:1–42. [PubMed: 15961057]
28. Margalit A, Duffin KL, Isakson PC. Rapid quantitation of a large scope of eicosanoids in two models of inflammation: development of an electrospray and tandem mass spectrometry method and application to biological studies. *Analytical biochemistry.* 1996; 235:73–81. [PubMed: 8850549]
29. Quehenberger O, Armando A, Dumlao D, Stephens DL, Dennis EA. Lipidomics analysis of essential fatty acids in macrophages. Prostaglandins, leukotrienes, and essential fatty acids. 2008; 79:123–129.
30. Deems R, Buczynski MW, Bowers-Gentry R, Harkewicz R, Dennis EA. Detection and quantitation of eicosanoids via high performance liquid chromatography-electrospray ionization-mass spectrometry. *Methods in enzymology.* 2007; 432:59–82. [PubMed: 17954213]
31. Buczynski MW, Stephens DL, Bowers-Gentry RC, Grkovich A, Deems RA, Dennis EA. TLR-4 and sustained calcium agonists synergistically produce eicosanoids independent of protein synthesis in RAW264.7 cells. *The Journal of biological chemistry.* 2007; 282:22834–22847. [PubMed: 17535806]
32. Blaho VA, Buczynski MW, Brown CR, Dennis EA. Lipidomic analysis of dynamic eicosanoid responses during the induction and resolution of Lyme arthritis. *The Journal of biological chemistry.* 2009; 284:21599–21612. [PubMed: 19487688]
33. Golovko MY, Murphy EJ. An improved LC-MS/MS procedure for brain prostanoid analysis using brain fixation with head-focused microwave irradiation and liquid-liquid extraction. *Journal of lipid research.* 2008; 49:893–902. [PubMed: 18187404]
34. Jian W, Edom R, Weng N, Zannikos P, Zhang Z, Wang H. Validation and application of an LC-MS/MS method for quantitation of three fatty acid ethanolamides as biomarkers for fatty acid hydrolase inhibition in human plasma. *Journal of chromatography.* 878:1687–1699.
35. Hall LM, Murphy RC. Electrospray mass spectrometric analysis of 5-hydroperoxy and 5-hydroxyeicosatetraenoic acids generated by lipid peroxidation of red blood cell ghost phospholipids. *Journal of the American Society for Mass Spectrometry.* 1998; 9:527–532. [PubMed: 9879367]

### The abbreviations used are

<b>NAE</b>	N-acylethanolamine
<b>sMRM</b>	scheduled multiple reaction monitoring
<b>LIPID MAPS</b>	LIPID Metabolites And Pathways Strategy
<b>AA</b>	arachidonic acid
<b>20:4; AEA</b>	anamide
<b>COX</b>	cyclooxygenase
<b>LOX</b>	lipoygenase

<b>CYP</b>	cytochrome P450
<b>15d-PGJ<sub>2</sub></b>	15-deoxy- $\Delta$ 12,14-PGJ <sub>2</sub>
<b>PGE<sub>2</sub></b>	prostaglandin E <sub>2</sub>
<b>PGD<sub>2</sub></b>	prostaglandin D <sub>2</sub>
<b>PGJ<sub>2</sub></b>	prostaglandin J <sub>2</sub>
<b>dhk-PGD<sub>2</sub></b>	13,14-dihydro-15-keto prostaglandin D <sub>2</sub>
<b>5-iso PGF<sub>2<math>\alpha</math></sub> IV</b>	5-iso-prostaglandin F <sub>2<math>\alpha</math></sub> IV
<b>5,6 EET-EA</b>	5,6-epoxy-eicosatetrienoic acid ethanolamide
<b>8,9EET-EA</b>	8,9-epoxy-eicosatetrienoic acid ethanolamide
<b>11,12 EET-EA</b>	11,12-epoxy-eicosatetrienoic acid ethanolamide
<b>14,15 EET-EA</b>	14,15-epoxy-eicosatetrienoic acid ethanolamide
<b>15-HETE-EA</b>	15-hydroxy-eicosapentaenoic acid ethanolamide
<b>PGF<sub>2<math>\alpha</math></sub>-EA</b>	prostaglandin F <sub>2<math>\alpha</math></sub> ethanolamide
<b>20:3-EA</b>	dihomo- $\gamma$ -linolenoyl ethanolamide
<b>16:0-EA</b>	lauroyl ethanolamide
<b>18:2-EA</b>	linoleoyl ethanolamide
<b>24:0-EA</b>	lignoceryl ethanolamide
<b>5-HETE</b>	5-hydroxy-eicosapentaenoic acid
<b>16-HETE</b>	16-hydroxy-eicosapentaenoic acid
<b>17-HETE</b>	17-hydroxy-eicosapentaenoic acid
<b>18-HETE</b>	18-hydroxy-eicosapentaenoic acid
<b>20-HETE</b>	20-hydroxy-eicosapentaenoic acid
<b>LTB<sub>4</sub></b>	Leukotriene B <sub>4</sub>
<b>9-HODE</b>	9-hydroxy-octadecatrienoic acid
<b>13-HODE</b>	13-hydroxy-octadecatrienoic acid
<b>9,10-diHOME</b>	9,10-dihydro-octadecenoic acid
<b>12,13-diHOME</b>	12,13-dihydro-octadecenoic acid

**Research Highlights**

> We present a high-throughput Lipidomics methodology for eicosanoids and N-acylethanolamines. > The rationale behind the method design is addressed. > Quantitation for 100 eicosanoid and 33 N-acylethanolamine species. > Limits of detections are determined. > Biological application of the methodology is demonstrated.



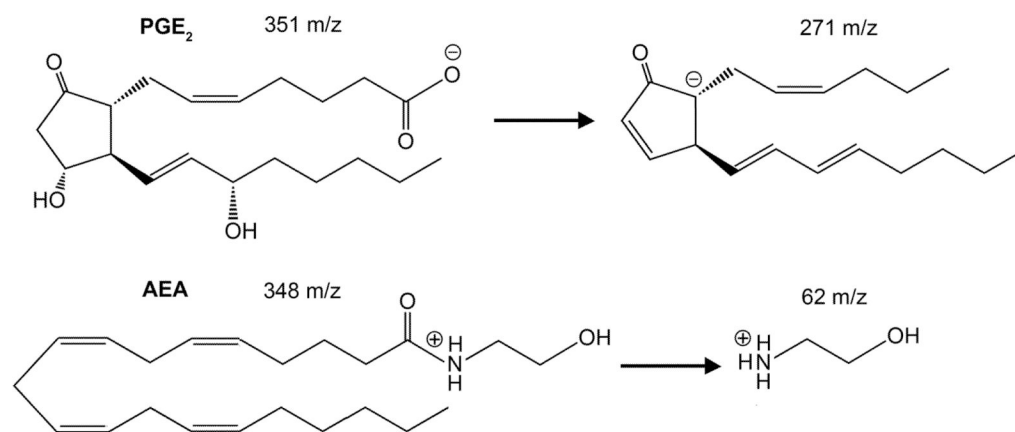


**Figure 1.** The structures of the parent and daughter ions for PGE<sub>2</sub> and AEA used in this method.

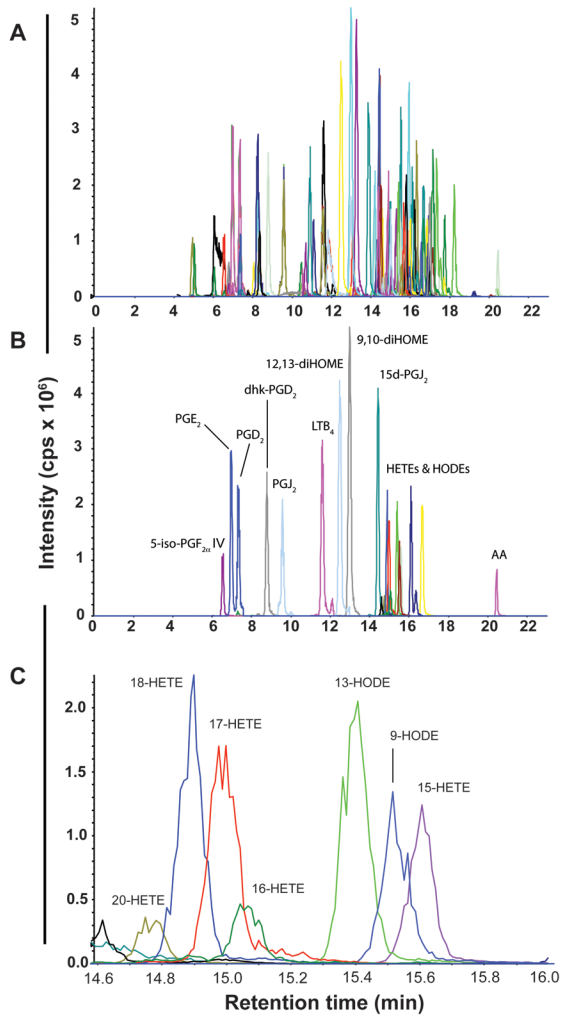


**Figure 2.** Chromatogram from a single 100 ng standard solution subjected to our eicosanoid methodology. (A) 102 sMRM pairs were extracted from a single run. (B) Selected eicosanoid sMRM pairs from the major biosynthetic pathways were extracted from a single analysis. (C) A magnified view of the chromatogram of extracted HETE and HODE metabolites.

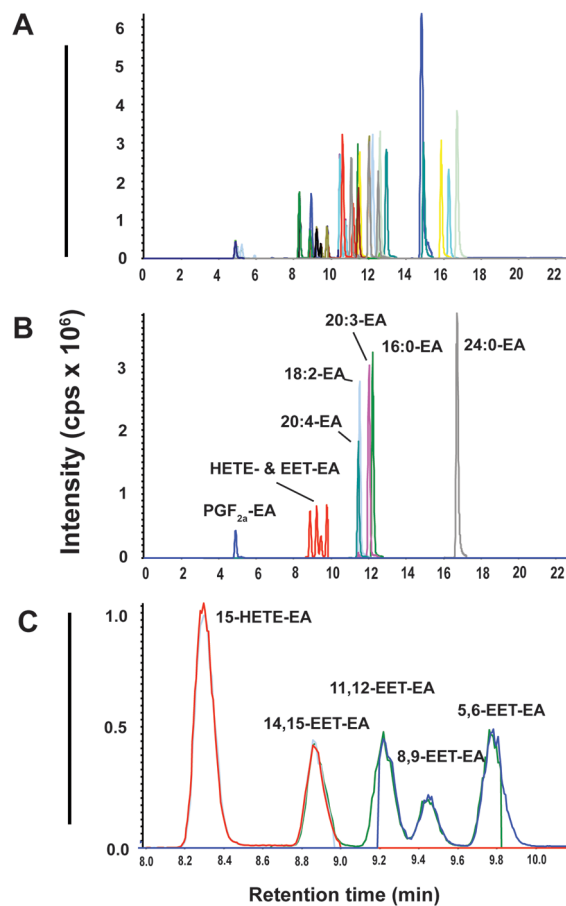


**Figure 3.** Chromatogram from a single 100 ng standard solution subjected to our ethanolamine methodology. (A) 40 sMRM pairs were extracted from a single run. (B) A diverse group of selected ethanolamides sMRM pairs were extracted from a single analysis. (C) A magnified view of the chromatogram of extracted HETE-EA and EET-EA metabolites.

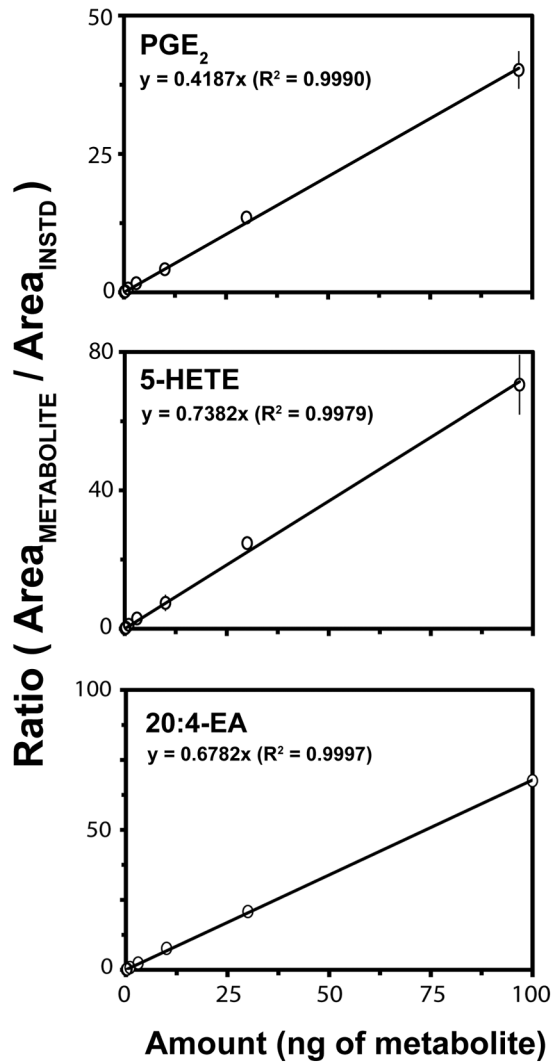


**Figure 4.** Primary standard curves from representative eicosanoid and ethanolamine metabolites were generated from 3 separate experiments performed in duplicate. Primary standard curves were generated from 7 concentrations ranging from 0.1 – 100 ng. Error bars represent the standard error of the mean.

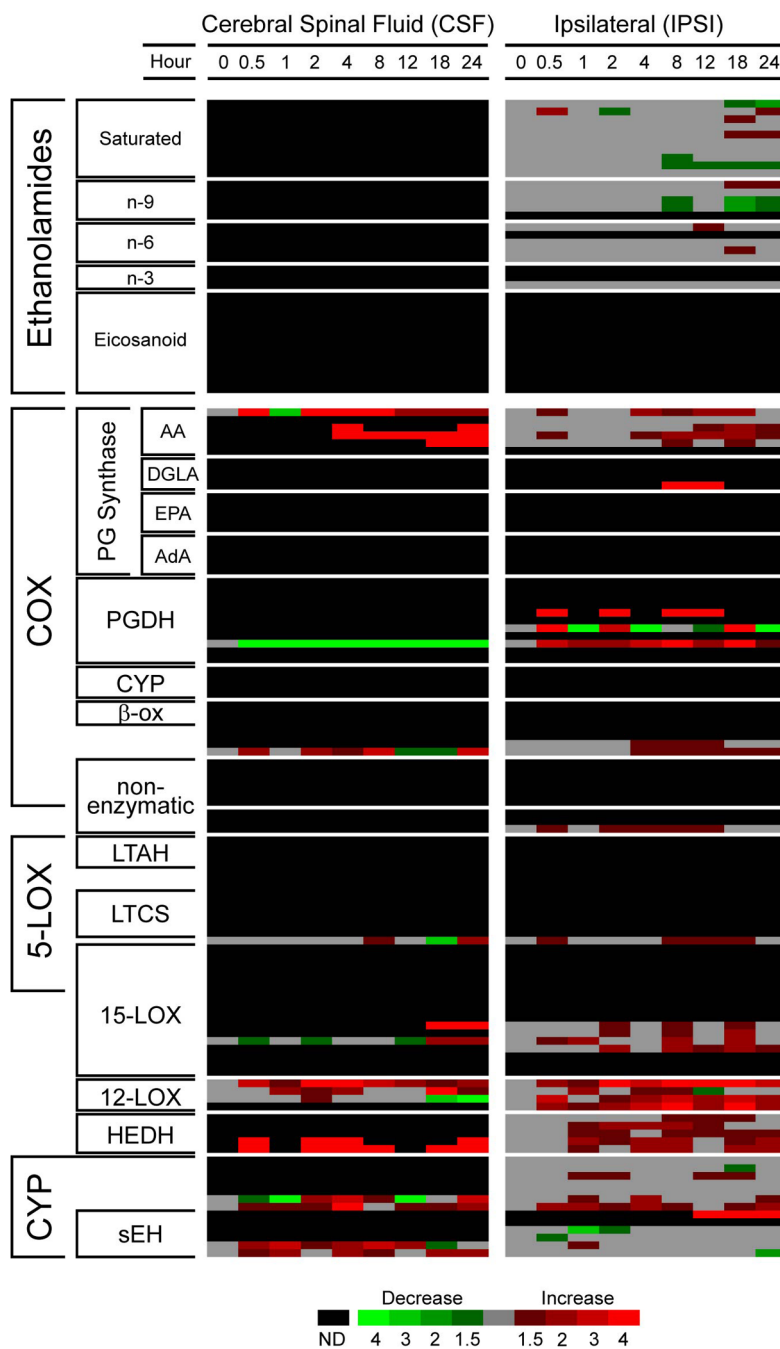


**Figure 5.** A time-course heat map of cerebral spinal fluid (CSF) and the ipsilateral of the portion lumbar spinal cord (IPST) from rats treated with the hyperalgesia-inducing agent carrageenan. Metabolites are clustered based on their biosynthetic pathway. This data is adapted from Buczynski *et al* (16).

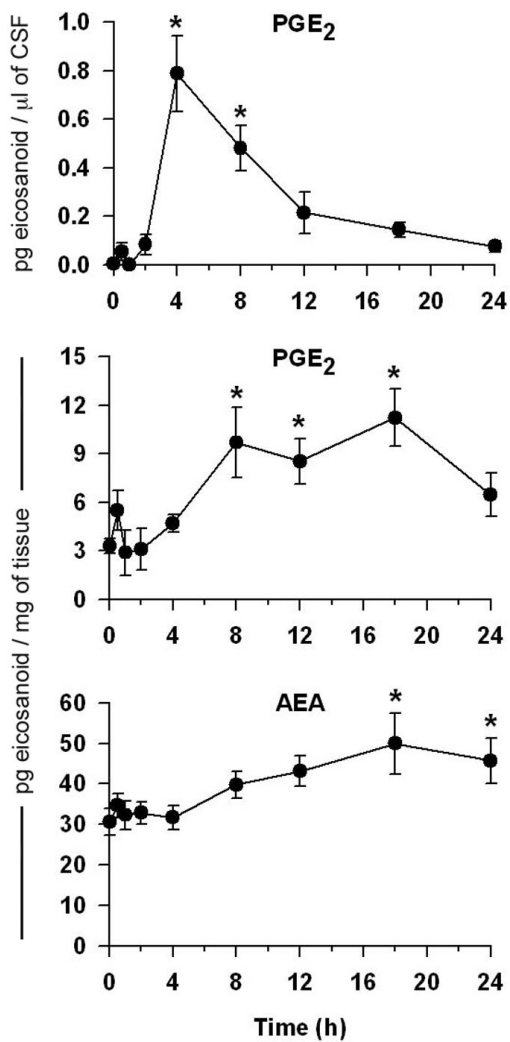


**Figure 6.** Quantitative amounts of eicosanoid and ethanolamine in CSF and spinal cord over a 24 h time-course. Error bars represent the standard error of the mean. \* indicate p-values < 0.05. This data is adapted from Buczynski *et al* (16).



Table 1

## Optimized sMRM pairs and parameters for eicosanoids

Fatty acid	Pathway	COMMON NAME	Abbreviation	Parent	Daughter	Retention Time (min) <sup>b</sup>	LOD (pg)	Declustering Potential	Collision Energy	Internal Standard
AA	COX	$\alpha$ -(d4) 6-keto-Prostaglandin F <sub>1a</sub>	(d4) 6k-PGF <sub>1a</sub>	373	167	5.0	ND	-65	-35	-
AA	COX	(d4) Thromboxane B <sub>2</sub>	(d4) TXB <sub>2</sub>	373	173	6.3	ND	-50	-25	-
AA	COX	(d4) Prostaglandin F <sub>2a</sub>	(d4) PGF <sub>2a</sub>	357	197	6.9	ND	-50	-30	-
AA	COX	(d4) Prostaglandin E <sub>2</sub>	(d4) PGE <sub>2</sub>	355	275	7.1	ND	-50	-25	-
AA	COX	(d4) Prostaglandin D <sub>2</sub>	(d4) PGD <sub>2</sub>	355	275	7.5	ND	-50	-25	-
AA	COX	(d4) 15-deoxy-Prostaglandin J <sub>2</sub>	(d4) 15d-PGJ <sub>2</sub>	319	275	14.5	ND	-60	-20	-
AA	COX	(d4) 13,14-dihydro-15-keto Prostaglandin F <sub>2a</sub>	(d4) dhk PGF <sub>2a</sub>	357	295	8.3	ND	-80	-30	-
AA	COX	(d4) 13,14-dihydro-15-keto Prostaglandin E <sub>2</sub>	(d4) dhk PGE <sub>2</sub>	355	211	8.0	ND	-45	-30	-
AA	COX	(d4) 13,14-dihydro-15-keto Prostaglandin D <sub>2</sub>	(d4) dhk PGD <sub>2</sub>	355	211	8.9	ND	-45	-30	-
AA	non-enz	(d11) Isoprostane F <sub>2a</sub> -IV	(d11) 5-iso PGF <sub>2a</sub> VI	364	115	6.6	ND	-60	-30	-
AA	LOX	(d4) Leukotriene B <sub>4</sub>	(d4) LTB <sub>4</sub>	339	197	11.6	ND	-70	-22	-
AA	LOX	(d8) 5-hydroxy-eicosatrienoic acid	(d8) 5-HETE	327	116	16.7	ND	-50	-20	-
AA	LOX	(d8) 12-hydroxy-eicosatrienoic acid	(d8) 12-HETE	327	183	16.1	ND	-60	-20	-
AA	LOX	(d8) 15-hydroxy-eicosatrienoic acid	(d8) 15-HETE	327	226	15.5	ND	-60	-20	-
AA	CYP	(d6) 20-hydroxy-eicosatrienoic acid	(d6) 20-HETE	325	295	14.7	ND	-70	-20	-
LA	LOX	(d4) 9-hydroxy-octadecadienoic acid	(d4) 9-HODE	299	172	15.6	ND	-60	-25	-
LA	LOX	(d4) 13-hydroxy-octadecadienoic acid	(d4) 13-HODE	299	198	15.4	ND	-60	-25	-
AA	LOX	(d7) 5-oxo-eicosatetraenoic acid	(d7) 5-oxoETE	323	209	17.2	ND	-50	-25	-
AA	LOX	(d4) Resolvin E <sub>1</sub>	(d4) RvE <sub>1</sub>	353	197	5.2	ND	-70	-20	-
AA	CYP	(d8) 5(6)-epoxy-eicosatrienoic acid	(d8) 5,6 EET	330	202	17.6	ND	-30	-20	-
AA	CYP	(d8) 8(9)-epoxy-eicosatrienoic acid	(d8) 8,9 EET	327	158	17.5	ND	-60	-20	-
AA	CYP	(d8) 11(12)-epoxy-eicosatrienoic acid	(d8) 11,12 EET	327	171	17.5	ND	-60	-20	-
AA	CYP	(d8) 14(15)-epoxy-eicosatrienoic acid	(d8) 14,15 EET	327	226	16.9	ND	-50	-15	-
LA	CYP	(d4) 9,10-dihydroxy-octadecenoic acid	(d4) 9,10 diHOME	317	203	13.0	ND	-60	-30	-
LA	CYP	(d4) 12,13-dihydroxy-octadecenoic acid	(d4) 12,13 diHOME	317	185	12.4	ND	-60	-30	-
AA	LOX	(d5) Leukotriene C <sub>4</sub>	(d5) LTC <sub>4</sub>	630	272	9.2	ND	-70	-35	-
AA	LOX	(d4) Leukotriene E <sub>4</sub>	(d4) LTE <sub>4</sub>	441	336	10.2	ND	-60	-25	-

Fatty acid	Pathway	COMMON NAME	Abbreviation	Parent	Daughter	Retention Time (min) <sup>b</sup>	LOD (pg)	Declustering Potential	Collision Energy	Internal Standard
-	-	(d8) Arachidonic acid	(d8) AA	311	267	20.6	ND	-80	-20	-
-	-	(d5) Eicosapentaenoic acid	(d5) EPA	306	262	19.3	ND	-65	-15	-
-	-	(d5) Docosahexaenoic acid	(d5) DHA	332	234	20.2	ND	-95	-20	-
AA	COX	6-keto-Prostaglandin F <sub>1α</sub>	6k-PGF <sub>1α</sub>	369	163	5.1	1	-65	-35	(d4) 6k-PGF <sub>1α</sub>
AA	COX	Thromboxane B <sub>2</sub>	TXB <sub>2</sub>	369	169	6.3	1	-50	-25	(d4) TXB <sub>2</sub>
AA	COX	Prostaglandin F <sub>2α</sub>	PGF <sub>2α</sub>	353	193	6.9	1	-50	-30	(d4) PGF <sub>2α</sub>
AA	COX	Prostaglandin E <sub>2</sub>	PGE <sub>2</sub>	351	271	7.1	1	-50	-25	(d4) PGE <sub>2</sub>
AA	COX	Prostaglandin D <sub>2</sub>	PGD <sub>2</sub>	351	271	7.5	1	-50	-25	(d4) PGD <sub>2</sub>
AA	COX	11-beta-Prostaglandin F <sub>2α</sub>	11β PGF <sub>2α</sub>	353	193	6.2	ND	-50	-30	(d4) PGF <sub>2α</sub>
DgLA	COX	Thromboxane B <sub>1</sub>	TXB <sub>1</sub>	371	171	6.1	ND	-50	-25	(d4) TXB <sub>2</sub>
DgLA	COX	Prostaglandin F <sub>1α</sub>	PGF <sub>1α</sub>	355	293	7.0	ND	-75	-30	(d4) PGF <sub>2α</sub>
DgLA	COX	Prostaglandin E <sub>1</sub>	PGE <sub>1</sub>	353	273	7.4	ND	-55	-25	(d4) PGE <sub>2</sub>
DgLA	COX	Prostaglandin D <sub>1</sub>	PGD <sub>1</sub>	353	273	7.5	ND	-55	-25	(d4) PGD <sub>2</sub>
EPA	COX	Δ17-6-keto-Prostaglandin F <sub>1α</sub>	Δ17 6k-PGF <sub>1α</sub>	367	163	4.4	ND	-90	-35	(d4) PGF <sub>2α</sub>
EPA	COX	Thromboxane B <sub>3</sub>	TXB <sub>3</sub>	367	169	5.3	ND	-50	-25	(d4) TXB <sub>2</sub>
EPA	COX	Prostaglandin F <sub>3α</sub>	PGF <sub>3α</sub>	351	193	5.8	ND	-75	-30	(d4) PGF <sub>2α</sub>
EPA	COX	Prostaglandin E <sub>3</sub>	PGE <sub>3</sub>	349	269	6.2	ND	-55	-25	(d4) PGE <sub>2</sub>
EPA	COX	Prostaglandin D <sub>3</sub>	PGD <sub>3</sub>	349	269	6.5	ND	-55	-25	(d4) PGD <sub>2</sub>
ADA	COX	dihomo Prostaglandin F <sub>2α</sub>	dihomo PGF <sub>2α</sub>	381	221	8.9	ND	-75	-35	(d4) PGF <sub>2α</sub>
ADA	COX	dihomo Prostaglandin E <sub>2</sub>	dihomo PGE <sub>2</sub>	379	299	9.1	ND	-65	-30	(d4) PGE <sub>2</sub>
ADA	COX	dihomo Prostaglandin D <sub>2</sub>	dihomo PGD <sub>2</sub>	379	299	9.4	ND	-65	-30	(d4) PGD <sub>2</sub>
ADA	COX	dihomo Prostaglandin J <sub>2</sub>	dihomo PGJ <sub>2</sub>	361	299	12.3	ND	-55	-25	(d4) 15d-PGJ <sub>2</sub>
ADA	COX	dihomo 15-deoxy-Prostaglandin J <sub>2</sub>	dihomo 15d PGJ <sub>2</sub>	361	299	13.9	ND	-55	-25	(d4) 15d-PGJ <sub>2</sub>
DgLA	COX	6-keto-Prostaglandin E <sub>1</sub>	6k PGE <sub>1</sub>	367	143	5.3	ND	-40	-25	(d4) PGE <sub>2</sub>
DgLA	COX	6,15-diketo-, 13,14-dihydro-Prostaglandin F <sub>1α</sub>	6,15 dk-dh-PGF <sub>1α</sub>	369	113	6.2	ND	-60	-40	(d4) PGF <sub>2α</sub>
DgLA	COX	15-keto-Prostaglandin F <sub>1α</sub>	15k PGF <sub>1α</sub>	353	113	7.4	ND	-50	-35	(d4) PGF <sub>2α</sub>
AA	COX	15-keto-Prostaglandin F <sub>2α</sub>	15k PGF <sub>2α</sub>	351	113	7.4	ND	-40	-35	(d4) PGF <sub>2α</sub>
AA	COX	15-keto-Prostaglandin E <sub>2</sub>	15k PGE <sub>2</sub>	349	113	7.5	1	-35	-30	(d4) PGE <sub>2</sub>
AA	COX	13,14-dihydro-Prostaglandin F <sub>2α</sub>	dh PGF <sub>2α</sub>	355	275	7.7	ND	-40	-25	(d4) PGF <sub>2α</sub>

Fatty acid	Pathway	COMMON NAME	Abbreviation	Parent	Daughter	Retention Time (min) <sup>b</sup>	LOD (pg)	Declustering Potential	Collision Energy	Internal Standard
AA	COX	13,14-dihydro-15-keto Prostaglandin F <sub>2α</sub>	dhk PGF <sub>2α</sub>	353	291	8.1	1	-60	-25	(d4) dhk PGF <sub>2α</sub>
AA	COX	13,14-dihydro-15-keto Prostaglandin E <sub>2</sub>	dhk PGE <sub>2</sub>	351	207	8.2	1	-40	-25	(d4) dhk PGE <sub>2</sub>
AA	COX	13,14-dihydro-15-keto Prostaglandin D <sub>2</sub>	dhk PGD <sub>2</sub>	351	207	8.9	1	-40	-25	(d4) dhk PGD <sub>2</sub>
AA	COX	bicyclo Prostaglandin E <sub>2</sub>	bicyclo PGE <sub>2</sub>	333	113	10.6	ND	-60	-35	(d4) PGE <sub>2</sub>
AA	COX	11beta-13,14-dihydro-15-keto-Prostaglandin F <sub>2α</sub>	11β dhk PGF <sub>2α</sub>	353	113	8.0	ND	-50	-35	(d4) PGF <sub>2α</sub>
AA	COX	19-hydroxy-PGF <sub>2α</sub>	19oh PGF <sub>2α</sub>	369	193	3.3	ND	-50	-35	(d4) PGF <sub>2α</sub>
AA	COX	20-hydroxy-PGF <sub>2α</sub>	20oh PGF <sub>2α</sub>	369	193	3.2	ND	-50	-35	(d4) PGF <sub>2α</sub>
AA	COX	19-hydroxy-PGE <sub>2</sub>	19oh PGE <sub>2</sub>	367	189	3.6	ND	-40	-25	(d4) PGE <sub>2</sub>
AA	COX	20-hydroxy-PGE <sub>2</sub>	20oh PGE <sub>2</sub>	367	189	3.5	ND	-40	-25	(d4) PGE <sub>2</sub>
AA	COX	2,3-dimor-11-beta-Prostaglandin F <sub>2α</sub>	2,3 dimor 11β PGF <sub>2α</sub>	325	145	5.2	ND	-40	-25	(d4) PGF <sub>2α</sub>
AA	COX	tetranor-Prostaglin F Metabolite	tetranor-PGFM	329	293	2.5	ND	-40	-25	(d4) PGF <sub>2α</sub>
AA	COX	tetranor-Prostaglandin E Metabolite	tetranor-PGEM	327	291	2.5	ND	-40	-25	(d4) PGE <sub>2</sub>
AA	LOX	tetranor 12-hydroxy-eicosatetraenoic acid	tetranor 12-HETE	265	109	13.0	0.1	-75	-14	(d8) 15-HETE
AA	COX	11-beta-Prostaglandin E <sub>2</sub>	11β PGE <sub>2</sub>	351	271	7.1	ND	-40	-25	(d4) PGE <sub>2</sub>
AA	COX	Prostaglandin K <sub>2</sub>	PGK <sub>2</sub>	349	205	7.1	ND	-50	-30	(d4) PGE <sub>2</sub>
AA	COX	12S-hydroxy-heptadecatrienoic acid	12-HHT	279	163	13.4	1	-30	-30	(d8) 5-HETE
AA	COX	11-hydroxy-eicosatetraenoic acid	11-HETE	319	167	16.0	0.1	-60	-20	(d8) 5-HETE
AA	COX	11-hydroxy-eicosapentaenoic acid	11-HEPE	317	121	14.8	1	-70	-24	(d8) 15-HETE
AA	COX	13-hydroxy-docosahexaenoic Acid	13-HDoHE	343	221	15.8	0.1	-60	-17	(d8) 15-HETE
AA	COX	Prostaglandin A <sub>2</sub>	PGA <sub>2</sub>	333	271	9.7	ND	-30	-20	(d4) 15d-PGJ <sub>2</sub>
AA	COX	Prostaglandin B <sub>2</sub>	PGB <sub>2</sub>	333	271	9.5	ND	-30	-20	(d4) 15d-PGJ <sub>2</sub>
AA	COX	15-deoxy-Prostaglandin A <sub>2</sub>	15d-PGA <sub>2</sub>	315	271	15.0	ND	-50	-15	(d4) 15d-PGJ <sub>2</sub>
AA	COX	Prostaglandin J <sub>2</sub>	PGJ <sub>2</sub>	333	271	9.7	1	-30	-20	(d4) 15d-PGJ <sub>2</sub>
AA	COX	15-deoxy-Δ12,14-PGD <sub>2</sub>	15d-PGD <sub>2</sub>	333	271	11.7	1	-30	-20	(d4) 15d-PGJ <sub>2</sub>
AA	COX	15-deoxy-Δ12,14-PGJ <sub>2</sub>	15d-PGJ <sub>2</sub>	315	271	14.5	0.1	-50	-15	(d4) 15d-PGJ <sub>2</sub>
AA	non-enz	Isoprostane F <sub>2α</sub> -IV	5-iso PGF <sub>2α</sub> VI	353	115	6.7	1	-60	-30	(d11) 5-iso PGF <sub>2α</sub> VI
AA	non-enz	Isoprostane F <sub>2α</sub> -III	8-iso PGF <sub>2α</sub> III	353	193	6.2	1	-50	-30	(d11) 5-iso PGF <sub>2α</sub> VI
AA	non-enz	9-hydroxy-eicosatetraenoic acid	9-HETE	319	151	16.5	0.1	-60	-20	(d8) 5-HETE
EPA	non-enz	9-hydroxy-eicosapentaenoic acid	9-HEPE	317	149	15.0	0.1	-75	-20	(d8) 5-HETE

Fatty acid	Pathway	COMMON NAME	Abbreviation	Parent	Daughter	Retention Time (min) <sup>b</sup>	LOD (pg)	Declustering Potential	Collision Energy	Internal Standard
DHA	non-enz	8-hydroxy-docosahexaenoic Acid	8-HDoHE	343	109	16.2	0.1	-70	-20	(d8) 5-HETE
DHA	non-enz	16-hydroxy-docosahexaenoic Acid	16-HDoHE	343	233	15.5	0.1	-75	-19	(d8) 15-HETE
DHA	non-enz	20-hydroxy-docosahexaenoic Acid	20-HDoHE	343	241	15.3	0.1	-60	-20	(d8) 15-HETE
AA	LOX	Leukotriene B <sub>4</sub>	LTB <sub>4</sub>	335	195	11.5	1	-70	-22	(d4) LTB <sub>4</sub>
AA	LOX	20-hydroxy-Leukotriene B <sub>4</sub>	20oh LTB <sub>4</sub>	351	195	5.1	ND	-60	-25	(d4) LTB <sub>4</sub>
AA	LOX	20-carboxy-Leukotriene B <sub>4</sub>	20cooh LTB <sub>4</sub>	365	195	5.1	ND	-60	-25	(d4) LTB <sub>4</sub>
AA	LOX	5,6 dihydroxy-eicosatetraenoic acid	5,6 diHETE	335	163	15.0	1	-60	-25	(d4) LTB <sub>4</sub>
AA	LOX	6-trans-Leukotriene B <sub>4</sub>	6t LTB <sub>4</sub>	335	195	11.1	ND	-70	-22	(d4) LTB <sub>4</sub>
AA	LOX	12-epi-Leukotriene B <sub>4</sub>	12epi LTB <sub>4</sub>	335	195	11.1	ND	-70	-22	(d4) LTB <sub>4</sub>
AA	LOX	6-trans-,12-epi-Leukotriene B <sub>4</sub>	6t,12epi LTB <sub>4</sub>	335	195	11.1	ND	-70	-22	(d4) LTB <sub>4</sub>
AA	LOX	12-oxo-Leukotriene B <sub>4</sub>	12-oxoLTB <sub>4</sub>	333	179	12.4	ND	-60	-17	(d4) LTB <sub>4</sub>
AA	LOX	Leukotriene C <sub>4</sub>	LTC <sub>4</sub>	625	272	9.2	ND	-70	-28	(d5) LTC <sub>4</sub>
AA	LOX	Leukotriene D <sub>4</sub>	LTD <sub>4</sub>	495	177	10.6	ND	-60	-25	(d4) LTE <sub>4</sub>
AA	LOX	Leukotriene E <sub>4</sub>	LTE <sub>4</sub>	438	333	10.2	1	-60	-25	(d4) LTE <sub>4</sub>
AA	LOX	11-trans-Leukotriene C <sub>4</sub>	11tLTC <sub>4</sub>	625	272	9.8	ND	-70	-35	(d5) LTC <sub>4</sub>
AA	LOX	11-trans-Leukotriene D <sub>4</sub>	11tLTD <sub>4</sub>	495	177	11.5	ND	-60	-25	(d4) LTE <sub>4</sub>
AA	LOX	11-trans-Leukotriene E <sub>4</sub>	11tLTE <sub>4</sub>	438	333	10.9	ND	-60	-25	(d4) LTE <sub>4</sub>
AA	LOX	5-hydroxy-eicosatetraenoic acid	5-HETE	319	115	16.6	0.1	-60	-20	(d8) 5-HETE
EPA	LOX	5-hydroxy-eicosapentaenoic acid	5-HEPE	317	115	15.3	0.1	-40	-17	(d8) 5-HETE
DHA	LOX	7-hydroxy-docosahexaenoic acid	7-HDoHE	343	141	16.2	0.1	-60	-18	(d8) 5-HETE
DHA	LOX	4-hydroxy-docosahexaenoic acid	4-HDoHE	343	101	16.8	0.1	-70	-17	(d8) 5-HETE
LA	LOX	9-hydroxy-octadecatrienoic acid	9-HOTE	293	171	14.1	0.1	-70	-20	(d8) 5-HETE
MA	LOX	5-hydroxy-eicosatrienoic acid	5-HETE	321	115	18.3	0.1	-70	-19	(d8) 5-HETE
AA	LOX	5S,15S-dihydroxy-eicosatetraenoic acid	5,15 diHETE	335	201	11.1	1	-50	-30	(d4) LTB <sub>4</sub>
AA	LOX	5(S),6(R)-Lipoxin A <sub>4</sub>	6R-LXA <sub>4</sub>	351	115	8.0	1	-30	-20	(d4) LTB <sub>4</sub>
AA	LOX	5(S),6(S)-Lipoxin A <sub>4</sub>	6S-LXA <sub>4</sub>	351	115	8.3	1	-30	-20	(d4) LTB <sub>4</sub>
AA	LOX	5(S),14(R)-Lipoxin A <sub>4</sub>	14R-LXA <sub>4</sub>	351	115	8.1	ND	-70	-25	(d4) LTB <sub>4</sub>
EPA	LOX	Lipoxin A <sub>5</sub>	LXA <sub>5</sub>	349	113	6.7	ND	-60	-25	(d4) LTB <sub>4</sub>
AA	LOX	Lipoxin B <sub>4</sub>	LXB <sub>4</sub>	351	221	7.3	ND	-80	-25	(d4) LTB <sub>4</sub>
EPA	LOX	Resolvin E <sub>1</sub>	RvE <sub>1</sub>	349	195	5.2	ND	-70	-20	(d4) RvE <sub>1</sub>

Fatty acid	Pathway	COMMON NAME	Abbreviation	Parent	Daughter	Retention Time (min) <sup>b</sup>	LOD (pg)	Declustering Potential	Collision Energy	Internal Standard
EPA	LOX	Resolvin D <sub>1</sub>	RvD <sub>1</sub>	375	141	7.8	ND	-45	-20	(d4) LTB <sub>4</sub>
DHA	LOX	Neuroprotectin D <sub>1</sub>	PD <sub>1</sub>	359	153	10.5	ND	-40	-20	(d4) LTB <sub>4</sub>
DHA	LOX	15-trans Neuroprotectin D <sub>1</sub>	15t PD <sub>1</sub>	359	153	10.8	ND	-40	-20	(d4) LTB <sub>4</sub>
DHA	LOX	10S,17S-dihydroxy Docosahexaenoic acid	10S,17S-DiHDoHE	359	153	11.0	ND	-40	-20	(d4) LTB <sub>4</sub>
AA	LOX	8S,15S-dihydroxy-eicosatetraenoic acid	8,15 diHETE	335	127	10.7	1	-50	-25	(d4) LTB <sub>4</sub>
AA	LOX	15-hydroxy-eicosatetraenoic acid	15-HETE	319	219	15.6	0.1	-50	-15	(d8) 15-HETE
EPA	LOX	15-hydroxy-eicosapentaenoic acid	15-HEPE	317	219	14.6	0.1	-60	-20	(d8) 5-HETE
DHA	LOX	17-hydroxy Docosahexaenoic acid	17-HDoHE	343	245	15.6	0.1	-60	-20	(d8)15-HETE
LA	LOX	13-hydroxy-octadecadienoic acid	13-HODE	295	195	15.4	1	-60	-25	(d4) 13-HODE
ALA	LOX	13-hydroxy-octadecatrienoic acid	13-HOTrE	293	195	14.3	1	-80	-25	(d4) 13-HODE
gLA	LOX	13-hydroxy-g-octadecatrienoic acid	13-HOTre-g	293	193	14.5	0.1	-70	-20	(d4) 13-HODE
DgLA	LOX	15-hydroxy-eicosatrienoic acid	15-HETE	321	221	16.3	0.1	-70	-21	(d8) 15-HETE
AA	LOX	8-hydroxy-eicosatetraenoic acid	8-HETE	319	155	16.3	0.1	-60	-20	(d8) 5-HETE
EPA	LOX	8-hydroxy-eicosapentaenoic acid	8-HEPE	317	127	14.9	1	-70	-25	(d8) 5-HETE
DHA	LOX	10-hydroxy Docosahexaenoic acid	10-HDoHE	343	181	15.8	1	-60	-17	(d8) 5-HETE
DgLA	LOX	8-hydroxy-eicosatrienoic acid	8-HEtrE	321	157	16.8	1	-70	-23	(d8) 5-HETE
AA	LOX	Eoxin C <sub>4</sub>	EXC <sub>4</sub>	625	272	7.2	ND	-70	-35	(d5) LTC <sub>4</sub>
AA	LOX	Eoxin D <sub>4</sub>	EXD <sub>4</sub>	495	177	10.7	ND	-60	-25	(d4) LTE <sub>4</sub>
AA	LOX	Eoxin E <sub>4</sub>	EXE <sub>4</sub>	438	333	8.7	ND	-60	-25	(d4) LTE <sub>4</sub>
AA	LOX	12-hydroxy-eicosatetraenoic acid	12-HETE	319	179	16.2	1	-60	-20	(d8) 15-HETE
EPA	LOX	12-hydroxy-eicosapentaenoic acid	12-HEPE	317	179	14.9	0.1	-70	-20	(d8) 15-HETE
DHA	LOX	14-hydroxy-docosahexaenoic acid	14-HDoHE	343	205	15.8	1	-60	-18	(d8) 15-HETE
DHA	LOX	11-hydroxy-docosahexaenoic acid	11-HDoHE	343	149	16.0	1	-60	-19	(d8) 5-HETE
LA	LOX	9-hydroxy-octadecadienoic acid	9-HODE	295	171	15.6	1	-60	-25	(d4) 9-HODE
AA	LOX	Hepoxilin A <sub>3</sub>	HXA <sub>3</sub>	335	127	14.3	1	-50	-25	(d8) 14,15 EET
AA	LOX	Hepoxilin B <sub>3</sub>	HXB <sub>3</sub>	335	183	14.4	1	-40	-20	(d8) 14,15 EET
AA	LOX	5-oxo-eicosatetraenoic acid	5-oxoETE	317	203	17.2	1	-40	-25	(d7) 5-oxoETE
AA	LOX	12-oxo-eicosatetraenoic acid	12-oxoETE	317	153	16.1	1	-40	-25	(d7) 5-oxoETE
AA	LOX	15-oxo-eicosatetraenoic acid	15-oxoETE	317	113	15.9	1	-40	-25	(d7) 5-oxoETE
LA	LOX	9-oxo-octadecadienoic acid	9-oxoODE	293	185	16.1	1	-60	-25	(d7) 5-oxoETE

Fatty acid	Pathway	COMMON NAME	Abbreviation	Parent	Daughter	Retention Time (min) <sup>b</sup>	LOD (pg)	Declustering Potential	Collision Energy	Internal Standard
LA	LOX	13-oxo-octadecadienoic acid	13-oxoODE	293	113	15.7	1	-70	-30	(d7) 5-oxoETE
EPA	LOX	15-oxo-eicosadienoic acid	15-oxoEDE	321	113	17.7	1	-100	-32	(d7) 5-oxoETE
AA	CYP	20-hydroxy-eicosatetraenoic acid	20-HETE	319	289	14.8	1	-75	-25	(d6) 20-HETE
AA	CYP	19-hydroxy-eicosatetraenoic acid	19-HETE	319	231	14.6	1	-80	-25	(d6) 20-HETE
AA	CYP	18-hydroxy-eicosatetraenoic acid	18-HETE	319	261	15.0	0.1	-80	-25	(d6) 20-HETE
AA	CYP	17-hydroxy-eicosatetraenoic acid	17-HETE	319	247	15.1	0.1	-80	-25	(d6) 20-HETE
AA	CYP	16-hydroxy-eicosatetraenoic acid	16-HETE	319	189	15.1	1	-80	-25	(d6) 20-HETE
EPA	CYP	18-hydroxy-eicosapentaenoic acid	18-HEPE	317	215	14.2	0.1	-60	-20	(d6) 20-HETE
AA	CYP	5(6)-epoxy-eicosathenoic acid	5,6 EET	319	191	17.8	1	-30	-20	(d8) 5,6 EET
AA	CYP	8(9)-epoxy-eicosatrienoic acid	8,9 EET	319	155	17.5	1	-60	-20	(d8) 8,9 EET
AA	CYP	11(12)-epoxy-eicosatrienoic acid	11,12 EET	319	167	17.3	1	-60	-20	(d8) 11,12 EET
AA	CYP	14(15)-epoxy-eicosatrienoic acid	14,15 EET	319	219	16.9	1	-50	-15	(d8) 14,15 EET
EPA	CYP	14,15-epoxy Eicosatetraenoic acid	14,15 EpETE	317	208	15.8	1	-65	-18	(d8) 14,15 EET
EPA	CYP	17,18-epoxy Eicosatetraenoic acid	17,18 EpETE	317	215	15.6	1	-65	-16	(d8) 14,15 EET
DHA	CYP	16,17-epoxy Docosapentaenoic acid	16,17 EpDPE	343	193	17.0	1	-70	-16	(d8) 14,15 EET
DHA	CYP	19,20-epoxy Docosapentaenoic acid	19,20 EpDPE	343	241	16.5	1	-70	-17	(d8) 14,15 EET
DHA	CYP	19,20-dihydroxy-docosapentaenoic acid	19,20 DiHDPA	361	229	13.1	1	-70	-25	(d8) 14,15 EET
LA	CYP	9(10)-epoxy-octadecenoic acid	9,10 EpOME	295	171	17.1	1	-60	-25	(d4) 9,10 diHOME
LA	CYP	12(13)-epoxy-octadecenoic acid	12,13 EpOME	295	195	17.1	1	-60	-25	(d4) 12,13 diHOME
AA	CYP	5,6-dihydroxy-eicosatrienoic acid	5,6 DHET	337	145	15.0	0.1	-75	-25	(d8) 5-HETE
AA	CYP	8,9-dihydroxy-eicosatrienoic acid	8,9 DHET	337	127	14.4	1	-60	-30	(d8) 5-HETE
AA	CYP	11,12-dihydroxy-eicosatrienoic acid	11,12 DHET	337	167	14.0	0.1	-60	-25	(d8) 5-HETE
AA	CYP	14,15-dihydroxy-eicosatrienoic acid	14,15 DHET	337	207	13.3	0.1	-60	-25	(d8) 5-HETE
LA	CYP	9,10-dihydroxy-octadecenoic acid	9,10 diHOME	313	201	12.9	0.1	-60	-30	(d4) 9,10 diHOME
LA	CYP	12,13-dihydroxy-octadecenoic acid	12,13 diHOME	313	183	12.4	1	-60	-30	(d4) 12,13 diHOME
-	-	Arachidonic acid	AA	303	259	20.6	ND	-80	-20	(d8) AA
-	-	Adrenic acid	ADA	331	287	21.3	ND	-80	-20	(d8) AA
-	-	Eicosapentaenoic acid	EPA	301	257	19.4	ND	-65	-15	(d5) EPA
-	-	Docohexaenoic acid	DHA	327	229	20.2	ND	-95	-20	(d5) DHA

<sup>a</sup> deturated internal standards are shaded in grey.

<sup>b</sup> retention time are representative values.



**Table 2**  
**Optimized sMRM pairs and parameters for N-acyl ethanolamines**

COMMON NAME	Abbreviation	Parent	Daughter	Retention Time (min) <sup>b</sup>	LOD (pg)	Internal Standard
<i>α</i> -(d4) Prostaglandin F <sub>2α</sub> Ethanamide	(d4) PGF <sub>2α</sub> -EA	384	62	5.1	ND	-
(d4) Palmitoyl Ethanamide	(d4) 16:0-EA	312	62	12.1	ND	-
(d4) Oleoyl Ethanamide	(d4) 18:1-EA	328	62	12.5	ND	-
(d8) Arachidonyl Ethanamide	(d8) 20:4-EA	356	62	11.4	ND	-
Prostaglandin F <sub>2α</sub> Ethanamide	PGF <sub>2α</sub> -EA	380	62	5.1	1,000	(d4) PGF <sub>2α</sub> -EA
11-β-Prostaglandin F <sub>2α</sub> Ethanamide	11β PGF <sub>2α</sub> -EA	380	62	4.8	ND	(d4) PGF <sub>2α</sub> -EA
8-iso-Prostaglandin F <sub>2α</sub> III Ethanamide	8-iso-PGF <sub>2α</sub> III-EA	380	62	4.7	100	(d4) PGF <sub>2α</sub> -EA
Prostaglandin E <sub>2</sub> Ethanamide	PGE <sub>2</sub> -EA	378	62	5.2	100	(d4) PGF <sub>2α</sub> -EA
Prostaglandin D <sub>2</sub> Ethanamide	PGD <sub>2</sub> -EA	378	62	5.4	10	(d4) PGF <sub>2α</sub> -EA
5(6)-Epoxy-Eicosatrienoic acid Ethanamide	5,6-EET-EA	346	62	9.8	1	(d4) PGF <sub>2α</sub> -EA
8(9)-Epoxy-Eicosatrienoic acid Ethanamide	8,9-EET-EA	346	62	9.4	10	(d4) PGF <sub>2α</sub> -EA
11(12)-Epoxy-Eicosatrienoic acid Ethanamide	11,12-EET-EA	346	62	9.2	1	(d4) PGF <sub>2α</sub> -EA
14(15)-Epoxy-Eicosatrienoic acid Ethanamide	14,15-EET-EA	346	62	8.9	1	(d4) PGF <sub>2α</sub> -EA
15-Hydroxy-Eicosatetraenoic acid Ethanamide	15-HETE-EA	346	62	8.4	0.1	(d4) PGF <sub>2α</sub> -EA
20-Hydroxy-Eicosatetraenoic acid Ethanamide	20-HETE-EA	346	62	7.6	0.1	(d4) PGF <sub>2α</sub> -EA
Lauroyl Ethanamide	12:0-EA	244	62	8.9	10	(d4) 16:0-EA
Myristoyl Ethanamide	14:0-EA	272	62	10.6	10	(d4) 16:0-EA
Pentadecanoyl Ethanamide	15:0-EA	286	62	11.4	0.1	(d4) 16:0-EA
Palmitoyl Ethanamide	16:0-EA	300	62	12.2	0.1	(d4) 16:0-EA
Heptadecanoyl Ethanamide	17:0-EA	314	62	12.9	0.1	(d4) 16:0-EA
Stearoyl Ethanamide	18:0-EA	328	62	13.7	0.1	(d4) 16:0-EA
Arachidoyl Ethanamide	20:0-EA	356	62	14.8	0.1	(d4) 16:0-EA
Tricosanoyl Ethanamide	23:0-EA	398	62	16.2	0.1	(d4) 16:0-EA
Lignoceroyl Ethanamide	24:0-EA	412	62	16.6	0.1	(d4) 16:0-EA
Palmitoleyl Ethanamide	16:1-EA	298	62	11.1	0.1	(d4) 18:1-EA
Oleoyl Ethanamide	18:1-EA	326	62	12.5	0.1	(d4) 18:1-EA
Docosanoyl Ethanamide	22:1-EA	382	62	14.9	0.1	(d4) 18:1-EA

COMMON NAME	Abbreviation	Parent	Daughter	Retention Time (min) <sup>b</sup>	LOD (pg)	Internal Standard
Nervonoyl Ethanolamide	24:1-EA	410	62	15.8	0.1	(d4) 18:1-EA
Linoleoyl Ethanolamide	18:2-EA	324	62	11.5	0.1	(d8) 20:4-EA
$\alpha$ -Linolenoyl Ethanolamide	18:3( $\omega$ )-EA	322	62	10.8	10	(d8) 20:4-EA
$\gamma$ -Linolenoyl Ethanolamide	18:3( $\gamma$ )-EA	322	62	10.4	100	(d8) 20:4-EA
Meadoyl Ethanolamide	20:3-EA	350	62	12.4	0.1	(d8) 20:4-EA
Dihomo- $\gamma$ -Linolenoyl Ethanolamide	20:3-EA (D $\gamma$ LA)	350	62	12	0.1	(d8) 20:4-EA
Arachidonoyl Ethanolamide	20:4-EA	348	62	11.4	0.1	(d8) 20:4-EA
Docosatetraenoyl Ethanolamide	22:4-EA	376	62	12.5	0.1	(d8) 20:4-EA
Eicosapentaenoyl Ethanolamide	20:5-EA	346	62	10.5	0.1	(d8) 20:4-EA
Docohexaenoyl Ethanolamide	22:6-EA	372	62	11.2	0.1	(d8) 20:4-EA

<sup>a</sup> deuterated internal standards are shaded in grey.

<sup>b</sup> retention time are representative values.